

# 碳酸钙循环煅烧—碳酸化吸收 CO<sub>2</sub> 的热力学分析

李英杰, 赵长遂

(东南大学 洁净煤发电及燃烧技术教育部重点实验室, 江苏 南京 210096)

**摘 要:** 针对 CaCO<sub>3</sub> 的煅烧/碳酸化反应(CCR)循环吸收 CO<sub>2</sub> 的方法, 基于 ASPEN PLUS 平台进行了热力学模拟。以增压循环流化床作为碳酸化反应器, 采用 O<sub>2</sub>/CO<sub>2</sub> 气氛下燃烧的常压循环流化床作为煅烧炉。根据系统吉布斯自由能最小原理计算了当碳酸化过程中的平均转化率为 0.7 和新鲜吸收剂添加量为 8 kg/s 时, 经过多次煅烧—碳酸化反应后系统脱碳效率为 74%, 排放烟气中的 CO<sub>2</sub> 浓度为 5.3% 及煅烧炉回收的 CO<sub>2</sub> 浓度为 95.6%, 并模拟出了排放烟气中的产物成分, 得出了烟气再循环比例与 O<sub>2</sub>/CO<sub>2</sub> 体积比的关系。同时计算了不同平均碳酸化转化率时吸收剂的添加量与脱碳效率和排放烟气中 CO<sub>2</sub> 体积浓度的关系。

**关 键 词:** ASPEN PLUS; 煅烧; 碳酸化; CO<sub>2</sub> 分离; 热力学

中图分类号: TQ534 文献标识码: A

## 引 言

近年来, 全球变暖的趋势已日益明显, 所带来的负面影响包括: 海平面上升与陆地淹没、气候带的移动、飓风加剧、植被迁徙与物种灭绝、洋流变化与厄尔尼诺频发等。作为主要的温室气体 CO<sub>2</sub> 正受到更多的关注。目前, 我国 CO<sub>2</sub> 排放量已居世界第二位, 预计到 2025 年将位居世界第一位, 约占世界 CO<sub>2</sub> 排放总量的 1/5, 其中由燃煤产生的 CO<sub>2</sub> 约占排放总量的 76%。在未来相当长的时期内, 我国以煤炭为主的能源格局不会改变, 火电耗煤占煤炭消费量比例也将逐步增长, 而由此导致的 CO<sub>2</sub> 排放问题将更加严重。采用廉价、资源丰富的矿物质吸收 CO<sub>2</sub> 是非常具有吸引力的方法<sup>[1]</sup>。而石灰石等钙基材料是满足条件的矿物质, 它们煅烧分解产生的氧化钙能够吸收 CO<sub>2</sub>, 而且储量丰富, 价格便宜, 分布广泛。Silaban 和 Harrison 以及 Shimizu 等人提出了利用石灰石作为高温吸收剂<sup>[2-3]</sup>, 进行煅烧/碳酸化反应

(CCR)循环吸收 CO<sub>2</sub>。在煅烧炉中石灰石煅烧分解成 CaO 同时回收产生的 CO<sub>2</sub>, 形成的 CaO 进入碳酸化反应器吸收 CO<sub>2</sub>, 产生的碳酸钙再进入煅烧炉进行分解, 循环吸收 CO<sub>2</sub>, 同时补充新鲜的石灰石, 排出过度使用而失活的吸收剂。为了提高煅烧炉内回收 CO<sub>2</sub> 的纯度, 煅烧所需热量由燃料通过 O<sub>2</sub>/CO<sub>2</sub> 循环燃烧提供。目前, 尚未针对该技术建立工业试验系统, 因此尝试通过热力学模拟软件 ASPEN PLUS 对 CaCO<sub>3</sub> 的 CCR 过程进行模拟, 以便对大型工业应用提供指导。

ASPEN PLUS 已成功应用于煤、生物质等的燃烧和气化领域, 得出了许多精确的模拟数据和结果<sup>[4-5]</sup>。Kinoshita 等人利用 ASPEN PLUS 在生物油制氢过程中模拟 CaO 吸收 CO<sub>2</sub> 的反应流程<sup>[6]</sup>, 预测出 H<sub>2</sub> 的纯度可达 95%。Barelli 等人在 CH<sub>4</sub> 重整制氢过程中应用 ASPEN PLUS 模拟 CaO 的碳酸化/煅烧反应吸收 CO<sub>2</sub>, 以提高 H<sub>2</sub> 纯度及减少 CO<sub>2</sub> 的排放<sup>[7]</sup>, 得出了最佳的 CH<sub>4</sub> 浓度和操作参数, 但在模拟中没有考虑碳酸化反应的转化率。Wang 等人应用 ASPEN PLUS 计算了石灰石 CCR 吸收循环流化床锅炉, 燃烧石油焦所产生的 CO<sub>2</sub> 流程中的质量平衡和能量平衡, 在计算中没有考虑碳酸化过程中的转化率, 也没有把石灰石作为循环物流<sup>[8]</sup>。

本文应用 ASPEN PLUS 12.1 平台, 以 ASPEN PLUS 内建经典模型为基础, 考虑了碳酸化过程中平均转化率的影响, 把 CaCO<sub>3</sub> 作为循环物流, 对 CaCO<sub>3</sub> 的 CCR 循环吸收 CO<sub>2</sub> 流程进行了热力学模拟。

## 1 模拟流程的建立

在模拟中采用增压循环流化床作为碳酸化反应

收稿日期: 2007-06-01; 修订日期: 2007-06-19

基金项目: 国家重点基础研究发展计划(973 计划)资助项目(2006CB705806); 江苏省高校研究生科技创新计划资助项目(JS06059); 东南大学优秀博士学位论文基金资助项目(X06040)

作者简介: 李英杰(1977-)男, 山东寿光人, 东南大学博士研究生。

器, 常压循环流化床作为煅烧炉。在碳酸化反应器和煅烧炉中分别燃烧 NX 煤和 FF 煤, 煤质分析如表 1 所示。基于质量守恒、能量守恒及热力学定律对流程中各个反应阶段选用相应模块进行模拟, 共有 12 个反应模块、25 股物流(输入物流 AIR、O<sub>2</sub> 等, 中间物流 PRO1 ~ PRO6 及 CaO 等, 输出物流 FLUE-GAS1 等)和 2 股热流(Q-HEAT1 和 Q-HEAT2)。模块所对应的模拟阶段如表 2 所示。在模拟中进行以下假设:

(1) 煤燃烧时先进行热解释放出挥发分和 2 产

生焦炭, 再燃烧且反应完全;

(2) 反应过程中不考虑压力损失;

(3) 各反应器温度分布均匀;

(4) 反应中的分离模块均能够实现气固或气液的完全分离;

(5) 反应中形成的 CaSO<sub>4</sub>、失活的 CaO 及灰等都被分离排出, 而不进入循环物流中, 虽然该假设实际上较难实现, 但有利于简化流程, 便于理论计算分析。

表 1 反应中所用煤的工业分析、元素分析及硫形态分析

| 标识 | 工业分析/%          |                 |                 | 元素分析/%          |                 |                 |                 | 硫组成/%             |                |                |                | 低位发热量/MJ·kg <sup>-1</sup> |
|----|-----------------|-----------------|-----------------|-----------------|-----------------|-----------------|-----------------|-------------------|----------------|----------------|----------------|---------------------------|
|    | M <sub>ad</sub> | A <sub>ad</sub> | V <sub>ad</sub> | C <sub>ad</sub> | H <sub>ad</sub> | O <sub>ad</sub> | N <sub>ad</sub> | S <sub>ad,t</sub> | S <sub>s</sub> | S <sub>p</sub> | S <sub>o</sub> |                           |
| NX | 1.29            | 28.98           | 25.06           | 53.63           | 2.50            | 10.84           | 0.68            | 3.37              | 0.06           | 2.16           | 1.15           | 22.53                     |
| FF | 0.69            | 18.92           | 6.68            | 73.87           | 1.71            | 3.82            | 1.27            | 0.41              | 0.01           | 0.27           | 0.13           | 27.87                     |

表 2 反应模块的类型、功能及所对应模拟流程

| 反应块名称       | 反应块类型  | 反应块功能                  | 对应模拟反应步骤     |
|-------------|--------|------------------------|--------------|
| DECOMP1 ~ 2 | RYIELD | 能够规定反应器的收率             | 煤分解成单分子成分    |
| COMBUST     | GIBBS  | 根据 Gibbs 自由能最小实现化学和相平衡 | 煤热解产物的燃烧反应   |
| REAC        | GIBBS  | 根据 Gibbs 自由能最小实现化学和相平衡 | 吸收剂的硫化、碳酸化反应 |
| SEP-CAR     | SEP    | 根据规定流率把物流分成多股出口物流      | 碳酸化反应器的气固分离  |
| SEP-CAL     | SSPLIT | 把物流分成不同类型的物流           | 煅烧反应炉的气固分离   |
| RECYCLE     | FSPLIT | 把物流分成多股相同类型的物流         | 煅烧炉的烟气再循环    |
| HEATX1 ~ 3  | HEATX  | 两股物流之间的换热              | 换热过程         |
| FLASH       | FLASH2 | 严格实现气液分离               | 把烟气中的水除去     |

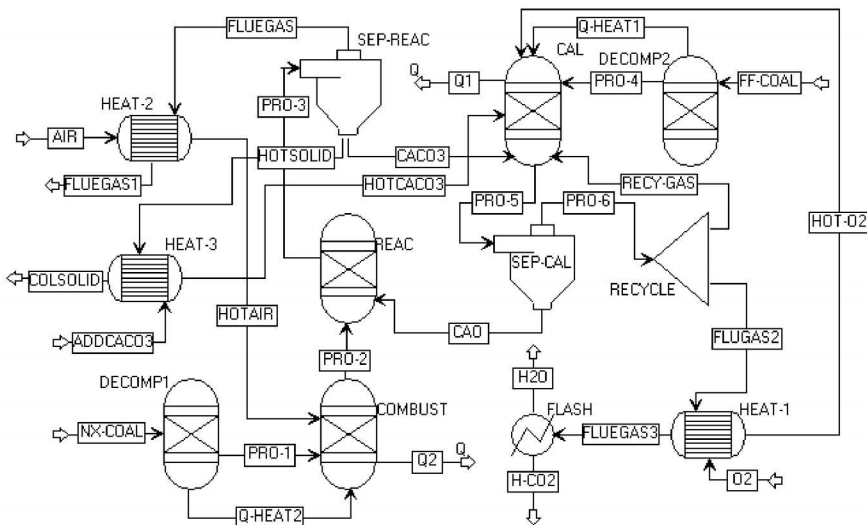


图 1 石灰石煅烧/碳酸化吸收 CO<sub>2</sub> 反应流程图

采用程序根据煤的工业分析和元素分析控制模块 RYIELD 各产物的量, 在煅烧炉中添加新鲜的  $\text{CaCO}_3$  以补偿失活的  $\text{CaO}$  和硫化消耗的  $\text{CaO}$ 。煅烧炉采用具有烟气再循环的  $\text{O}_2/\text{CO}_2$  气氛燃烧, 通过调整 FSPLIT 模块的再循环烟气比例  $\beta$  控制  $\text{O}_2/\text{CO}_2$  的体积比。流程中主要参数输入如下: NX 煤流量为 5 kg/s, 过量空气系数为 1.1, 燃烧空气量为 36.7 kg/s; FF 煤流量为 3 kg/s,  $\text{O}_2$  量为 6.75 kg/s; 初始循环  $\text{CaCO}_3$  物流为 16 kg/s; REAC、SULF、CAR 模块的反应温度为 850 °C, 压力为 2 MPa, CAR 模块的反应转化率  $X_{\text{ave}}$  为 0 ~ 1, CAL 模块中新鲜  $\text{CaCO}_3$  的添加量  $M_{\text{freshCaCO}_3}$  为 0 ~ 14 kg/s,  $0 < \beta < 1$ 。

## 2 $\text{CaCO}_3$ 煅烧后的碳酸化特性分析

$\text{CaCO}_3$  的 CCR 循环吸收  $\text{CO}_2$  反应中, 随着循环反应次数的增加, 吸收剂最大碳酸化能力逐渐下降, 转化率  $X_N$  逐渐降低<sup>[9]</sup>, 吸收剂的碳酸化能力逐渐衰减, 这主要是由于烧结作用, 使吸收剂的孔隙结构发生变化。  $X_N$  可表示为:

$$X_N = \frac{M_{N, \text{CaCO}_3}}{M_{0, \text{CaCO}_3}} \quad (3)$$

式中:  $N$ —循环反应次数;  $M_{0, \text{CaCO}_3}$ —初始  $\text{CaCO}_3$  的质量,  $M_{N, \text{CaCO}_3}$ —经过  $N$  次 CCR 循环后所形成的  $\text{CaCO}_3$  质量。 Abanndes 等人通过研究多种不同石灰石经过多次 CCR 后的  $X_N$  发现<sup>[10]</sup>:

$$X_N = f_m^N (1 - f_w) + f_w \quad (4)$$

式中:  $f_m$  和  $f_w$ —0.77 和 0.17。由式(4)不难发现, 经过 15 次循环反应后  $X_N$  为 0.19, 可见多次反应后  $X_N$  将降到较低的程度, 不利于  $\text{CO}_2$  的脱除。为了提高石灰石经多次 CCR 后的  $X_N$ , Hughes 等人在石灰石煅烧后又一定条件下水合<sup>[11]</sup>, 再进行碳酸化反应, 结果在进行了 20 次 CCR 循环后  $X_N$  可达 0.6。 Salvador 等人使用 NaCl 等添加剂调质石灰石<sup>[12]</sup>, 经过 15 次 CCR 后  $X_N$  为 0.5 左右。在加压条件下, 可获得比常压更高的  $X_N$ 。炉内总压力  $P_T$  与  $\text{CO}_2$  脱除效率  $E_{\text{CO}_2, \text{eq}}$  的关系<sup>[13]</sup>:

$$E_{\text{CO}_2, \text{eq}} = 1 - \frac{P_{\text{eq}}(1 - v_{\text{CO}_2})}{v_{\text{CO}_2}(P_T - P_{\text{eq}})} \quad (5)$$

式中:  $v_{\text{CO}_2}$ —烟气中  $\text{CO}_2$  的体积分数;  $P_{\text{eq}}$ —碳酸化温度对应的平衡分压力。当碳酸化温度为 850 °C 时的  $E_{\text{CO}_2, \text{eq}}$  经计算如图 2 所示。

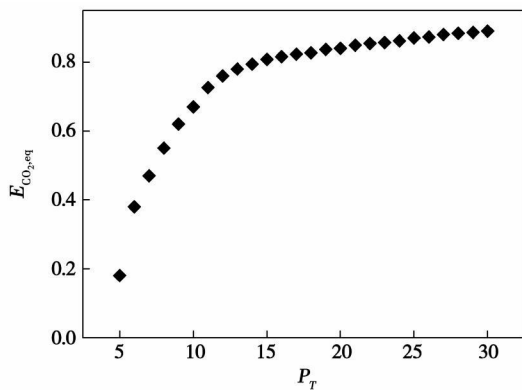


图 2  $E_{\text{CO}_2, \text{eq}}$  与  $P_T$  关系曲线

在碳酸化反应器中有新鲜的吸收剂加入, 又有失活吸收剂的排出同时还有继续循环反应的吸收剂。因此反应器的转化率是平均转化率  $X_{\text{aver}}$ :

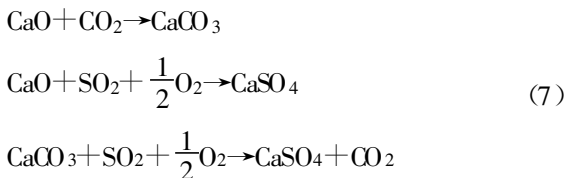
$$X_{\text{aver}} = \frac{\sum_{N=1}^{\infty} R_N X_N}{\sum_{N=1}^{\infty} R_N} \quad (6)$$

式中:  $R_N$ —第  $N$  次循环时进入碳酸化反应器内的吸收剂的质量分数。

## 3 基于 ASPEN PLUS 的流程模拟及分析

### 3.1 $X_{\text{aver}}$ 为 0.7 时的流程分析

在碳酸化反应中, REAC 模块选取  $X_{\text{aver}}$  为 0.7 进行计算, 假定  $M_{\text{freshCaCO}_3}$  为 8 kg/s。调整烟气再循环比例  $\beta$  为 0.65 时, 进入 CAL 模块的气体  $\text{O}_2/\text{CO}_2$  体积比为 21/79。NX 煤燃烧后的气体产物如表 3 所示,  $\text{CO}_2$  在烟气中的比例高达 17.2%。在 REAC 模块内反应较为复杂, 可能反应式如下:



采用 Gibbs 自由能最小的原理, 计算反应后烟气成分如表 4 所示。

表 3 NX 煤的燃烧产物 (kg/s)

| $\text{CO}_2$ | $\text{H}_2\text{O}$ | $\text{O}_2$ | $\text{NO}_x$ | $\text{N}_2$ | $\text{SO}_2$ | Ash  |
|---------------|----------------------|--------------|---------------|--------------|---------------|------|
| 9.7           | 1.17                 | 0.49         | 0.001         | 26.88        | 0.33          | 1.43 |

表 4 REAC 模块排放烟气成分 (kg/s)

| $\text{CO}_2$ | $\text{N}_2$ | $\text{H}_2\text{O}$ | $\text{O}_2$ | $\text{NO}_x$ | $\text{SO}_2$ |
|---------------|--------------|----------------------|--------------|---------------|---------------|
| 2.55          | 26.88        | 1.17                 | 0.41         | 0.001         | $< 10^{-4}$   |

由表4不难发现,经碳酸化后CO<sub>2</sub>量有了较大幅度的下降,CO<sub>2</sub>在排放烟气中的体积比 $r_{\text{CO}_2}$ 为5.3%,为了描述CO<sub>2</sub>脱除的程度,给出脱碳率 $E_{\text{CO}_2}$ 的定义:

$$E_{\text{CO}_2} = (M_{0,\text{CO}_2} - M_{1,\text{CO}_2}) / M_{1,\text{CO}_2} \quad (8)$$

式中: $M_{0,\text{CO}_2}$ —碳酸化反应器燃料燃烧后产生的CO<sub>2</sub>质量流; $M_{1,\text{CO}_2}$ —碳酸化反应器加入吸收剂后的CO<sub>2</sub>质量流。此时的 $E_{\text{CO}_2}$ 为74%。

对比表3和表4,SO<sub>2</sub>因为硫化反应的发生也大幅下降,同时硫化反应也消耗了一定的O<sub>2</sub>。采用GIBBS模块描述硫化反应,形成的CaSO<sub>4</sub>为0.76 kg/s。在模拟中忽略了宏观动力学因素的影响,如气固反应时的扩散等因素。另外,形成的CaSO<sub>4</sub>覆盖在CaO表面,可能阻碍CO<sub>2</sub>通过产物层的扩散,限制了碳酸化转化率,硫化对碳酸化的影响程度还要通过试验分析。

煅烧炉采用O<sub>2</sub>/CO<sub>2</sub>燃烧方式。从煅烧炉流出的CaO物流中CaO为13.43 kg/s,含FF煤的燃烧产生的灰分为0.56 kg/s,还混有一部分CaSO<sub>4</sub>为0.052 kg/s,主要是由在煅烧炉内部分煅烧产物CaO与FF煤的燃烧产物SO<sub>2</sub>反应而成的。煅烧炉排放烟气成分如表5所示,除水后回收的CO<sub>2</sub>的体积浓度可达95.6%。

表5 煅烧炉排放烟气成分 (kg/s)

| CO <sub>2</sub> | O <sub>2</sub> | NO <sub>x</sub> | N <sub>2</sub> | SO <sub>2</sub>    |
|-----------------|----------------|-----------------|----------------|--------------------|
| 18.62           | 0.58           | 0.001           | 0.038          | < 10 <sup>-4</sup> |

在 $X_{\text{aver}}$ 为0.7时,改变 $M_{\text{freshCaCO}_3}$ , $E_{\text{CO}_2}$ 和 $r_{\text{CO}_2}$ 都会发生改变。如图3所示,随着 $M_{\text{freshCaCO}_3}$ 的增大, $E_{\text{CO}_2}$ 呈增长趋势, $r_{\text{CO}_2}$ 则递减,且当 $M_{\text{freshCaCO}_3}$ 为12 kg/s时, $E_{\text{CO}_2}$ 接近90%,而 $r_{\text{CO}_2}$ 仅为2.9%。不难发现, $M_{\text{freshCaCO}_3}$ 为8 kg/s时是转折点,当 $M_{\text{freshCaCO}_3} > 8$  kg/s时, $E_{\text{CO}_2}$ 与 $M_{\text{freshCaCO}_3}$ 呈线性变化,当 $M_{\text{freshCaCO}_3} < 8$  kg/s时,也表现出近似的线性关系,但变化率要比前者大。在不同的 $M_{\text{freshCaCO}_3}$ 时,存在折线趋势的原因主要是因为当 $M_{\text{freshCaCO}_3}$ 小于8 kg/s时,由于初始循环CaCO<sub>3</sub>物流和添加新鲜的CaCO<sub>3</sub>一起煅烧形成的CaO,在转化率的影响下碳酸化反应所生成的CaCO<sub>3</sub>量小于初始循环物流量为16 kg/s的CaCO<sub>3</sub>,从而使整个煅烧/碳酸化反应在新的CaCO<sub>3</sub>循环物流量下进行。

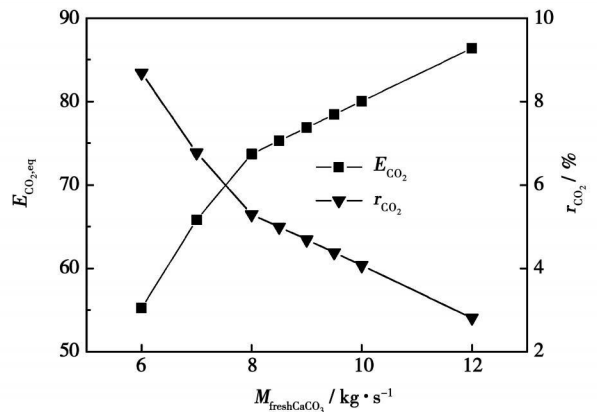


图3 不同 $M_{\text{freshCaCO}_3}$ 时的 $E_{\text{CO}_2}$ 和 $r_{\text{CO}_2}$

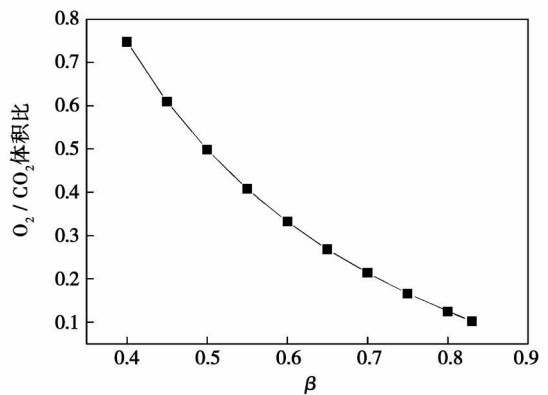


图4 再循环比例 $\beta$ 与O<sub>2</sub>/CO<sub>2</sub>体积比的关系

在 $X_{\text{aver}}$ 为0.7时 $M_{\text{freshCaCO}_3}$ 为8 kg/s条件下,在煅烧炉内反应过程中,计算RECYCLE模块的烟气再循环比例 $\beta$ 与O<sub>2</sub>/CO<sub>2</sub>体积比的关系,计算结果如图4所示。当煅烧炉内煤种改变时,则 $\beta$ 与O<sub>2</sub>/CO<sub>2</sub>体积比的关系也相应改变。根据计算结果,如果使进入煅烧炉内的O<sub>2</sub>/CO<sub>2</sub>体积比分别为30/70和40/60,则需分别调整 $\beta$ 为0.54和0.43。

### 3.2 不同 $X_{\text{aver}}$ 下的 $E_{\text{CO}_2}$ 和 $r_{\text{CO}_2}$

选择不同的碳酸化过程中平均转化率 $X_{\text{aver}}$ ,在 $X_{\text{aver}}$ 为0.7的研究基础上,再考察 $X_{\text{aver}}$ 分别为1.0、0.9、0.8和0.6对 $E_{\text{CO}_2}$ 和 $r_{\text{CO}_2}$ 的影响。如图5和图6所示,各个平均转化率下,随着 $M_{\text{freshCaCO}_3}$ 的增大, $r_{\text{CO}_2}$ 逐渐降低,变化趋势的形状为两条斜率不同的直线构成,存在转折点;而随 $M_{\text{freshCaCO}_3}$ 的增大, $E_{\text{CO}_2}$ 也增长,变化趋势与 $r_{\text{CO}_2}$ 的相反。当 $M_{\text{freshCaCO}_3}$ 小于转折点值时,导致碳酸化后形成的CaCO<sub>3</sub>量小于初始循环物流CaCO<sub>3</sub>的量,进而使整个流程的Ca元素量减小,导致 $r_{\text{CO}_2}$ 增大和 $E_{\text{CO}_2}$ 降低。改变在相同的 $r_{\text{CO}_2}$ 下, $X_{\text{aver}}$ 越高, $M_{\text{freshCaCO}_3}$ 也越小,如图7所示,要使 $r_{\text{CO}_2}$ 降低为

5%, 当  $X_{aver}$  为 0.9 时,  $M_{freshCaCO_3}$  仅需 3 kg/s, 而当  $X_{aver}$  为 0.6 时, 则需  $M_{freshCaCO_3}$  为 12.5 kg/s, 约为  $X_{aver}$  为 0.9 时的 4.2 倍。由此可见, 提高  $X_{aver}$  对于  $CaCO_3$  的 CCR 循环吸收  $CO_2$  过程而言是关键的。

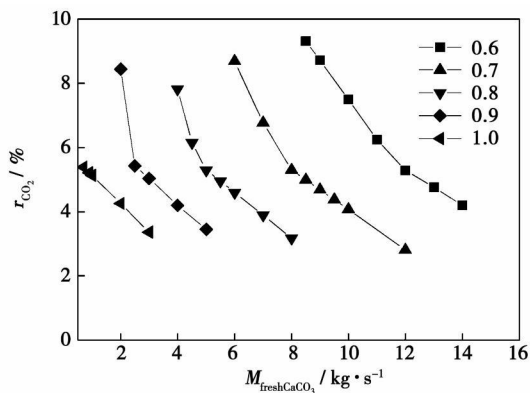


图 5 不同  $X_{aver}$  下  $M_{freshCaCO_3}$  与  $r_{CO_2}$  关系曲线

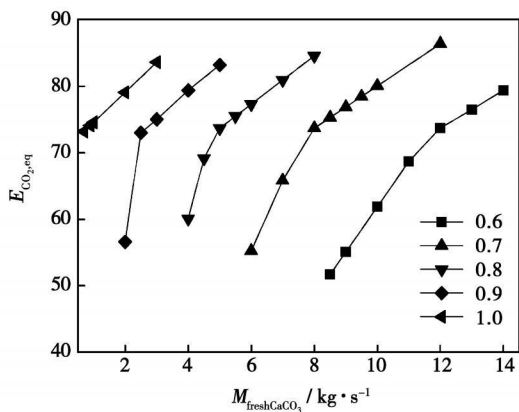


图 6 不同  $X_{aver}$  下  $M_{freshCaCO_3}$  与  $E_{CO_2}$  关系曲线

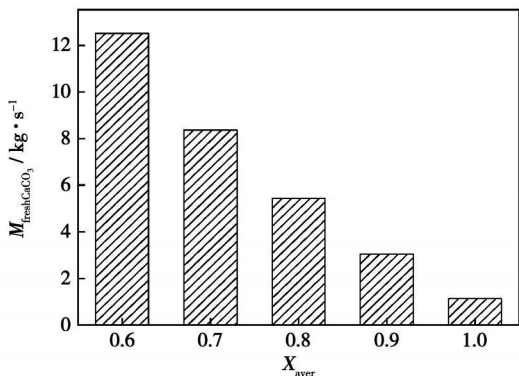


图 7 在  $r_{CO_2}$  为 5% 时的  $M_{freshCaCO_3}$  与  $X_{aver}$  关系曲线

## 4 结论

基于 ASPEN PLUS 平台, 以增压流化床作为碳酸化反应器, 采用  $O_2/CO_2$  燃烧方式的常压循环流化床作为煅烧炉, 在一定的平均碳酸化转化率下, 模拟

$CaCO_3$  的 CCR 多次循环吸收  $CO_2$  过程, 得出了烟气再循环比例与  $O_2/CO_2$  体积比的关系; 并根据不同转化率得出了  $CaCO_3$  的添加量与脱碳效率和烟气中  $CO_2$  浓度的关系, 随新鲜石灰石量的增大, 脱碳效率增大, 同时排放烟气中  $CO_2$  减小, 均呈折线变化, 存在转折点, 要提高燃煤锅炉脱碳效率关键是提高碳酸化过程的平均转化率。应用 ASPEN PLUS 平台计算可以为钙基吸收剂的循环煅烧/碳酸化分离  $CO_2$  过程提供理论指导。

## 参考文献:

- [1] ABANADES J C, RUBIN E S, ANTHONY E J. Sorbent Cost and Performance in  $CO_2$  Capture Systems[J]. Ind Eng Chem Res, 2004, 43(13): 3462-3466.
- [2] SILABAN A, HARRISON P. High temperature capture of carbon dioxide; characteristics of the reversible reaction between  $CaO(s)$  and  $CO_2(g)$ [J]. Chem Eng Comm, 1995, 137(7): 177-190.
- [3] SHIMIZU T, HIRAMA T, HOSODA H, et al. A twin fluid-bed reactor for removal of  $CO_2$  from combustion processes[J]. Trans I Chem E, 1999, 77(1): 62-68.
- [4] MATHIEU P, DUBUSSION R. Performance analysis of a biomass gasifier[J]. Energy Conversion & Management, 2002, 43(9-12): 1291-1299.
- [5] 李英杰, 赵长遂, 段伦博.  $O_2/CO_2$  气氛下煤燃烧产物的热力学分析[J]. 热能动力工程, 2007, 22(3): 332-335.
- [6] WANG J S, ANTHONY E, ABANADES C J. A simulation study for fluidized bed combustion of petroleum coke with  $CO_2$  capture // Proceedings of FBC2003 17th International Fluidized Bed Combustion Conference[C]. USA; Jacksonville, 2003: 1-4.
- [7] BARELLI L, BIDINI G, CORRADIETTI A. Production of hydrogen through the carbonation-calcination reaction applied to  $CH_4/CO_2$  mixtures[J]. Energy, 2007, 32(5): 543-552.
- [8] KINOSHITA M C, TURN S Q. Production of hydrogen from bio-oil using  $CaO$  as a  $CO_2$  sorbent[J]. International Journal of Hydrogen Energy, 2003, 28(10): 1065-1071.
- [9] MESS D, SAROFIM A F, LONGWELL J P. Product layer diffusion during the reaction of Calcium Oxide with Carbon Dioxide[J]. Energy and Fuels, 1999, 13(5): 999-1005.
- [10] ABANADES J C, ALVAREZ D. Conversion Limits in the reaction of  $CO_2$  with lime[J]. Energy and Fuels, 2003, 17(2): 308-315.
- [11] HUGHES R W, LU D, ANTHONY E J, et al. Improved long-term conversion of lime stone-derived sorbents for in situ capture of  $CO_2$  in a fluidized bed combustor[J]. Ind Eng Chem Res, 2004, 43(18): 5529-5539.
- [12] SALVADOR C, LU D, ANTHONY E J, et al. Enhancement of  $CaO$  for  $CO_2$  capture in an FBC environment[J]. Chemical Engineering Journal, 2003, 96(1-3): 187-195.
- [13] ANTHONY E J, WANG J S. Capturing  $CO_2$  in coal-fired combustors using  $CaO$ -based sorbents // In: Xu Xuchang, ed. Proc of the 5th Int Symposium of Coal Combustion[C]. Nanjing: Southeast University Press, 2003. 20-25.

(编辑 滨)

某船用锅炉过热器蒸汽与烟气传热流动数值模拟 = Numerical Simulation of Steam and Flue-gas Heat Transfer Flows in a Marine Boiler Superheater [刊, 汉] / CHEN Ming, CUI Xiao-li (No. 703 Research Institute of CSIC, Harbin, China, Post Code: 150036), LI Bang, GUI Hong-tao (College of Power and Energy Engineering, Harbin Engineering University, Harbin, China, 150001) // Journal of Engineering for Thermal Energy & Power. — 2008, 23(3). — 298 ~ 302

An integral three-dimensional numerical simulation was conducted for the turbulent flow of inner steam and outer flue gases of a marine boiler superheater. In the light of the structural features of the superheater, a special software Gambit was used to conduct a three dimensional geometric modeling and mesh division. A numerical simulation was performed by using software Fluent. A variety of distribution laws governing the steam flow fields were obtained, including the distribution of static pressure, flow rate and heat load as well as superheater tube-wall temperature field distribution. The simulation results are in relatively good agreement with the actual operating conditions of the superheater, thus providing valuable guidance for the structural design of marine boiler superheaters. **Key words:** superheater, steam flow, flue gas flow, temperature field, numerical simulation

湿法烟气脱硫喷淋塔不同喷嘴布置雾化性能比较试验 = Tests for Comparing the Atomization Performance of a Wet-method Flue-gas Desulfuration Spray Tower at Different Nozzle Arrangements [刊, 汉] / LI Zhao-dong (Nanjing Audit University, Nanjing, China, Post Code: 210029), YAN Lu, WANG Shi-he (Municipal Engineering Department, Southeast University, Nanjing, China, 210096), WANG Xiao-ming (National Power Environmental Protection Research Institute, Nanjing, China, 210031) // Journal of Engineering for Thermal Energy & Power. — 2008, 23(3). — 303 ~ 305

The spray tower represents a tower type most widely used in a wet-method flue gas desulfuration process and its atomization system pertains to a key technology of the spray tower, which influences the desulfuration mass transfer process. To conduct a more comprehensive study of the atomization performance of the spray tower, a test stand was set up. With the pressure serving as an indirect index, both the swirl and spiral nozzles commonly used in the wet-method desulfuration process were adopted. A comparison of the atomization performance of the spray tower has been conducted, using the following layouts, namely, single-layer/double-layer swirl nozzle arrangement, single-layer/double-layer spiral nozzle arrangement, swirl and spiral nozzle combined arrangement. The test results show that the role played by the atomization system on the gas flow distribution in the tower is not quite evident. By comparison, the upper swirl and lower spiral nozzle combined arrangement mode is the preferred choice for the atomization system in the tower, which can meet the requirements both for the process liquid-gas ratio and achieve a relatively good uniformity of the atomized particle distribution on the section and mist droplet dispersion on the spray section. **Key words:** flue gas desulfuration, spray tower, atomization performance, sectional pressure distribution

碳酸钙循环煅烧-碳酸化吸收 CO<sub>2</sub> 的热力学分析 = Thermodynamic Analysis of CO<sub>2</sub> Absorbed in the Process of Calcium Carbonate Cyclic Calcination/Carbonation [刊, 汉] / LI Ying-jie, ZHAO Chang-sui (Education Ministry Key Laboratory on Clean Coal Power Generation and Combustion Technology, Southeast University, Nanjing, China, Post Code: 210096) // Journal of Engineering for Thermal Energy & Power. — 2008, 23(3). — 306 ~ 310

A thermodynamic simulation was conducted on an Aspen Plus platform by using a method based on a cyclic absorption of carbon dioxide in the calcination/carbonation reaction of calcium carbonate. With a supercharged circulating fluidized bed serving as a carbonation reactor, a normal-pressure circulating fluidized bed was used as a calcination furnace featuring combustion in an atmosphere of O<sub>2</sub>/CO<sub>2</sub>. On the basis of the Gibbs free energy minimization theory when the average conversion rate is 0.7 and the amount of fresh absorbent added in the carbonation process is 8 kg/s, the system decarbonization efficiency was calculated as 74%, the CO<sub>2</sub> concentration in the discharged flue gas as 5.3% and the CO<sub>2</sub> concentration recovered from the calcination furnace as 95.6% as a result of repeated calcination/carbonation reactions. Moreover, simulated were the constituents of product in the discharged flue gas. As a result, the relationship between the flue gas recirculation proportion and O<sub>2</sub>/CO<sub>2</sub> volumetric ratio was obtained. In the meantime, the relationship among the amount of

absorbent added, the decarbonation efficiency and the CO<sub>2</sub> volumetric concentration in the discharged flue gas was calculated at different average carbonation conversion rates. **Key words:** Aspen Plus, calcination, carbonation, CO<sub>2</sub> separation

非等温柴油液滴对流蒸发的热膨胀与环境压力影响分析 = **Heat Expansion Caused by Convective Evaporation of Non-isothermal Diesel Oil Droplets and Analysis of its Effect on Ambient Pressure** [刊, 汉] / SUN Feng-xi-an, JIANG Ren-qiu (College of Power and Energy Engineering, Harbin Engineering University, Harbin, China, Post Code: 150001) // Journal of Engineering for Thermal Energy & Power. — 2008, 23(3). — 311 ~ 315

Based on a model for a non-isothermal liquid droplet evaporation with inner temperature gradient and heat expansion being taken into account, studied through a numerical simulation were the heat expansion caused by diesel oil droplet evaporation in a hot convection atmosphere and its effect on ambient pressure. Under the condition of considering the thermo-physical properties of liquid droplets and gas flow being under momentary changes with their temperature, pressure and constituents, through calculations, the curves showing the change in evaporation droplet radius in different hot atmospheres were obtained along with a comparison of the difference in the predicted results of droplet evaporation whether the heat expansion is taken into account or not. The research results show that there exists an obvious heat expansion in the convective evaporation process of diesel oil droplets, which can cause the life of liquid droplets to be shortened by over 10%. The effect of the ambient pressure exhibits a non-monotonous nature and may reverse under certain hot environmental conditions. **Key words:** non-isothermal liquid droplet, diesel oil, convective evaporation, heat expansion, ambient pressure

间接内重整固体氧化物燃料电池的建模与仿真 = **Modeling and Simulation of the Fuel Cell of an Indirect Internally Reformed Solid-oxide** [刊, 汉] / WANG Jin-li, ZHANG Hui-sheng, WENG Shi-lie (Education Ministry Key Laboratory on Turbo-machinery and Engineering, Shanghai Jiaotong University, Shanghai, China, Post Code: 200240) // Journal of Engineering for Thermal Energy & Power. — 2008, 23(3). — 316 ~ 320

A one-dimensional dynamic mathematic model was established for a fuel cell based on a catalytic-coating reformer and featuring an indirect internally reformed solid oxide. On the basis of the constituents and energy conservation and with an electrochemical model being taken into account, a simulation model of the fuel cell in question was established based on the distributed-lumped parameter technology and modularization concept. The model under discussion can not only reflect the distribution parameter characteristics of the fuel cell but also meet the demand for dynamic simulation. The steady-state performance of a SOFC (solid-oxide fuel cell) was analyzed at an operating condition and the simulation of a dynamic process was conducted by using the model in question. The research results show that the model can reflect the basic performance of the indirect internally reformed SOFC. **Key words:** indirect internally reformed SOFC (solid oxide fuel cell), catalytic coating reformer, distributed-lumped parameter, modeling, simulation

生物质/煤粉微量给料的实现与优化 = **Implementation and Optimization of Biomass/Pulverized Coal Micro-feeding** [刊, 汉] / XU Xiang-qian, GONG Zhi-qiang, LU Chun-mei, ZHANG Meng-zhu (College of Energy Source and Power Engineering, Shandong University, Jinan, China, Post Code: 250061) // Journal of Engineering for Thermal Energy & Power. — 2008, 23(3). — 321 ~ 323

To solve a variety of problems occurring in small-sized reburning test stands when pulverized coal and biomass are micro-fed, such as proneness to get sticky and clogged, non-uniform feeding and low accuracy, a two-wire screw-rod type feeder of pulverized coal was used to conduct a micro-feeding test. For pulverized coal/biomass of a small and large particle diameter, various methods, such as pre-drying and adding silicon gel powder in an amount of 5%—10% by weight and shaking at special locations, were adopted respectively to avoid the occurrence of agglomeration and rivulet flow phenomena, meet the requirement to limit the pulverized coal feeding rate at less than 1 g/min, and greatly improve the continuity and uniformity of the feeding. The feeding rate is usually within a range of 4% above or below the averaged rate. The methods under discussion feature high accuracy and good repeatability. **Key words:** micro-feeding, pulverized coal, biomass particle, spiral feeder, inertial additive